Short period La/B and LaN/B multilayer mirrors for ~6.8 nm wavelength

Igor A. Makhotkin,[1,2,*] Erwin Zoethout,[1] Robbert van de Kruijs,[1] Sergey N. Yakunin,[3] Eric Louis,[1,2] A. M. Yakunin,[4] V. Banine,[4] S. Müllender,[5] and Fred Bijkerk[1,2]

[1]FOM Institute DIFFER - Dutch Institute for Fundamental Energy Research, Nieuwegein, Netherlands
[2]MESA + Institute for Nanotechnology, University of Twente, Enschede, Netherlands
[3]NRC Kurchatov Institute, Moscow, Russia
[4]ASML, Veldhoven, Netherlands
[5]Carl Zeiss SMT, Oberkochen, Germany
[*]I.Makhotkin@utwente.nl

Abstract: In the first part of this article we experimentally show that contrast between the very thin layers of La and B enables close to theoretical reflectance. The reflectivity at 6.8 nm wavelength was measured from La/B multilayer mirrors with period thicknesses ranging from 3.5 to 7.2 nm at the appropriate angle for constructive interference. The difference between the measured reflectance and the reflectance calculated for a perfect multilayer structure decreases with increasing multilayer period. The reflectance of the multilayer with the largest period approaches the theoretical value, showing that the optical contrast between the very thin layers of these structures allows to experimentally access close to theoretical reflectance. In the second part of the article we discuss the structure of La/B and LaN/B multilayers. This set of multilayers is probed by hard X-rays (λ = 0.154 nm) and EUV radiation (λ = 6.8 nm). The structure is reconstructed based on a simultaneous fit of the grazing incidence hard X-ray reflectivity and the EUV reflectivity curves. The reflectivity analysis of the La/B and LaN/B multilayer mirrors shows that the lower reflectance of La/B mirrors compared to LaN/B mirrors can be explained by the presence of 5% of La atoms in the B layer and 63% of B in La layer. After multi-parametrical optimization of the LaN/B system, including the nitridation of La, the highest near normal incidence reflectivity of 57.3% at 6.6 nm wavelength has been measured from a multilayer mirror, containing 175 bi-layers. This is the highest value reported so far.

© 2013 Optical Society of America

OCIS codes: (340.7480) X-rays, soft x-rays, extreme ultraviolet (EUV); (340.7470) X-ray mirrors.

References and links

1. Y. Y. Platonov, L. Gomez, and D. Broadway, "Status of small d-spacing x-ray multilayers development at Osmic," Proc. SPIE **4782**, 152 (2002).
2. T. Tsarfati, E. Zoethout, R. W. E. van de Kruijs, and F. Bijkerk, "Nitridation and contrast of B_4C/La interfaces and multilayers," Thin Solid Films **518**(24), 7249–7252 (2010).
3. S. Andreev, M. Barysheva, N. Chkhalo, S. Gusev, A. Pestov, V. Polkovnikov, D. Rogachev, N. Salashchenko, Y. Vainer, and S. Zuev, "Multilayer X-ray mirrors based on La/B4C and La/B9C," Tech. Phys. **55**(8), 1168–1174 (2010).
4. I. A. Makhotkin, E. Zoethout, E. Louis, A. M. Yakunin, S. Müllender, and F. Bijkerk, "Spectral properties of La/B--based multilayer mirrors near the boron K absorption edge," Opt. Express **20**(11), 11778–11786 (2012).
5. T. Tsarfati, R. W. E. van de Kruijs, E. Zoethout, E. Louis, and F. Bijkerk, "Reflective multilayer optics for 6.7 nm wavelength radiation sources and next generation lithography," Thin Solid Films **518**(5), 1365–1368 (2009).
6. M. Barthelmess and S. Bajt, "Thermal and stress studies of normal incidence Mo/B4C multilayers for a 6.7 nm wavelength," Appl. Opt. **50**(11), 1610–1619 (2011).

#197545 - $15.00 USD Received 13 Sep 2013; revised 14 Nov 2013; accepted 20 Nov 2013; published 26 Nov 2013

7. C. Michaelsen, J. Wiesmann, R. Bormann, C. Nowak, C. Dieker, S. Hollensteiner, and W. Jäger, "Multilayer mirror for x rays below 190 eV," Opt. Lett. **26**(11), 792–794 (2001).
8. J. M. André, P. Jonnard, C. Michaelsen, J. Wiesmann, F. Bridou, M. F. Ravet, A. Jerome, F. Delmotte, and E. O. Filatova, "La/B4C small period multilayer interferential mirror for the analysis of boron," XRay Spectrom. **34**(3), 203–206 (2005).
9. V. Domnich, S. Reynaud, R. A. Haber, and M. Chhowalla, "Boron Carbide: Structure, Properties, and Stability under Stress," J. Am. Ceram. Soc. **94**(11), 3605–3628 (2011).
10. V. I. Gushenets, A. Hershcovitch, T. V. Kulevoy, E. M. Oks, K. P. Savkin, A. V. Vizir, and G. Y. Yushkov, "Boron ion source based on planar magnetron discharge in self-sputtering mode," Rev. Sci. Instrum. **81**(2), 02B303 (2010).
11. D. L. Windt, "IMD - Software for modeling the optical properties of multilayer films," Comput. Phys. **12**(4), 360–370 (1998).
12. M. Fernández-Perea, J. I. Larruquert, J. A. Aznárez, J. A. Méndez, M. Vidal-Dasilva, E. Gullikson, A. Aquila, R. Soufli, and J. L. G. Fierro, "Optical constants of electron-beam evaporated boron films in the 6.8-900 eV photon energy range," J. Opt. Soc. Am. A **24**(12), 3800–3807 (2007).
13. R. Soufli, A. L. Aquila, F. Salmassi, M. Fernández-Perea, and E. M. Gullikson, "Optical constants of magnetron-sputtered boron carbide thin films from photoabsorption data in the range 30 to 770 eV," Appl. Opt. **47**(25), 4633–4639 (2008).
14. S. S. Andreev, M. M. Barysheva, N. I. Chkhalo, S. A. Gusev, A. E. Pestov, V. N. Polkovnikov, N. N. Salashchenko, L. A. Shmaenok, Y. A. Vainer, and S. Y. Zuev, "Multilayered mirrors based on La/B4C(B9C) for X-ray range near anomalous dispersion of boron (lambda approximate to 6.7 nm)," Nuclear Instruments & Methods in Physics Research Section a-Accelerators Spectrometers Detectors and Associated Equipment **603**, 80-82 (2009).
15. E. Louis, A. E. Yakshin, T. Tsarfati, and F. Bijkerk, "Nanometer interface and materials control for multilayer EUV-optical applications," Prog. Surf. Sci. **86**(11-12), 255–294 (2011).
16. F. Scholze, C. Laubis, C. Buchholz, A. Fischer, S. Ploeger, F. Scholz, H. Wagne, and G. Ulm, "Status of EUV reflectometry at PTB," Proc. SPIE **5751**, 749–758 (2005).
17. A. E. Yakshin, R. W. E. van de Kruijs, I. Nedelcu, E. Zoethout, E. Louis, and F. Bijkerk, "Enhanced reflectance of interface engineered Mo/Si multilayers produced by thermal particle deposition," Proc. SPIE **6517**, 65170I (2007).
18. W. H. Press, *Numerical Recipes 3rd Edition: The Art of Scientific Computing* (Cambridge University, 2007).
19. M. Born and E. Wolf, *Principles of Optics,* Seventh ed. (Cambridge University, 2000).
20. I. A. Makhotkin, "Structural and reflective characteristics of mutllayers for 6.x nm wavelength," (University of Twente, Enschede, 2013).
21. J. F. Seely, Y. A. Uspenskii, B. Kjornrattanawanich, and D. L. Windt, "Coated photodiode technique for the determination of the optical constants of reactive elements: La and Tb," Proc. SPIE **6317**, 63170T (2006).

1. Introduction

One of the possible wavelengths for the next generation EUV lithography is around 6.8 nm [1–4]. To maximize the multilayer reflectance it is required to select materials with the highest possible optical contrast and the lowest possible absorption for the selected wavelength. The most commonly used multilayer material combinations for normal incidence reflectance at this wavelength, just above the boron K_α absorption edge, are Mo/B_4C or La/B_4C [1, 5].

Due to their good thermal stability, Mo/B_4C multilayer mirrors are often considered for applications using high power soft X-ray light sources, for example X-ray free electron lasers [6]. However, according to their bulk optical properties, La-based multilayers show a higher reflectance than Mo-based multilayers and are therefore better candidates for applications that require a high photon transmission such as EUV lithography. La/B_4C multilayer mirrors have also been studied for application in X-ray fluorescence spectroscopy [7], in particular for boron detection [8].

To increase the multilayer reflectivity further, B_4C should be replaced by boron since this is the optically preferable material in combination with La. The boron rich compound B_4C has been selected previously over boron because of its higher electrical conductivity [9] which simplifies deposition with commonly used DC magnetron sputtering techniques. Boron, being a semi-conductor at room temperature, is usually deposited by RF magnetron sputtering, but DC magnetron sputtering sources can be employed for boron when the target is heated above 400°C [10], where the conductivity improves sufficiently.

#197545 - $15.00 USD Received 13 Sep 2013; revised 14 Nov 2013; accepted 20 Nov 2013; published 26 Nov 2013
(C) 2013 OSA

Normal incidence reflectance calculations made with IMD [11], using measured optical constants for B [12] and B_4C [13], assuming a typical 0.3 nm rms roughness value for each interface and 200 period multilayers, show that La/B can reflect 7% more at 6.8 nm wavelength compared to La/B_4C. Reflectivity gain by replacing B_4C by B is experimentally demonstrated for 50 period La/B_4C and La/B multilayers with a period of 3.5 nm showing 7% and 10% normal incidence reflectance at $\lambda = 7$ nm respectively.

However, replacement of B_4C with a more boron rich boron-carbide is not always beneficial for reflectivity. Andreev et. al. [14] reported 38% reflectivity for La/B_9C multilayer mirrors, lower than the 44% reflectivity reported for La/B_4C in the same work. This boron-carbide example shows that differences in growth properties of the different materials can have a large impact on optical performance and may negate any theoretically expected improvements.

In the first part of this paper we discuss the potential of the optical contrast of the La/B material combination to reach high EUV reflectance by analysing the measured EUV reflectivity from multilayer stacks with different period thickness for various angles of incidence.

The second part of the paper describes the current state of our La/B- based multilayer mirrors. It has been reported that nitridation of La in La/B_4C multilayer mirrors increases the multilayer reflectivity [2]. This increase is assumed to be caused by the nitrogen passivation of the lanthanum preventing or mitigating lanthanum-boride formation. This can also be applied when B is used instead of B_4C. We will present the reflectivity and analysis of the structure of La/B and LaN/B stacks deposited for normal incidence of 6.8 nm EUV radiation. Here we analyse the multilayer structures in order to study the structural effects of the lanthanum nitridation in B based multilayers. We compare two ways of La nitridation: N-ion post treatment of the La layers and reactive magnetron sputtering of La using a N_2 and Ar gas mixture.

2. Optical contrast between La and B layers

In this paragraph we will discuss the reflectance of 40 period La/B multilayer stacks with different period thicknesses. To avoid run-to-run variations in the deposition process, all samples have been deposited in one deposition run, using a vapour-mask to vary the deposition flux. The mask enables the deposition of multilayer stacks with periods ranging from 7.8 nm to 3.2 nm. To minimize shadowing effects and simplify the mask design the electron beam evaporation technique has been used. Deposition is controlled using in situ soft X-ray reflectivity of C-K radiation from the sample in the centre of the substrate holder [15].

The multilayers have been characterized using at-wavelength reflectometry at the Physikalisch Technische Bundesanstalt (PTB) in Berlin [16] using radiation of the electron storage ring BESSY. The angle of incidence, given with respect to the surface normal, is selected to have the maximum reflectance at 6.8 nm for each sample. The results are presented in Table 1 and plotted in Fig. 1. We compare the measured reflectivity to the theoretical maximum reflectivity that is calculated for a model of 40 periods La/B without interface roughness, using bulk values for La and B densities and the as-deposited ratio of the La and B layer thickness. Figure 1 shows that the difference between calculated and measured curves decreases with the increase of the thickness of the multilayer period.

The decreasing discrepancy between measured and simulated reflectivity for higher period thickness can be attributed to the influence of interface imperfections. The reflectivity loss caused by interface roughness or intermixture can be described by multiplying the reflectivity from an interface without roughness by the Debye Waller-like correction factor $\exp(-q^2\sigma^2)$, were q is the scattering vector equal to $4\pi\cos(\theta)/\lambda$ (θ is angle of incidence (AOI) with respect to surface normal, λ is the X-ray wavelength) and σ is an effective interface thickness. According to Bragg's law in its basic form, so without taking the material optical constants into account, the scattering vector q is for the first order reflection equal to $2\pi/\Lambda$, where Λ is

#197545 - $15.00 USD Received 13 Sep 2013; revised 14 Nov 2013; accepted 20 Nov 2013; published 26 Nov 2013
(C) 2013 OSA

the multilayer period. This indicates that for multilayers with a larger period thickness and the same roughness σ, a lower reflectance loss due to roughness can be expected. Therefore, increasing the period thickness and measuring the reflectivity at a more grazing incidence angle, the effect of interfaces on the EUV reflectivity is minimized.

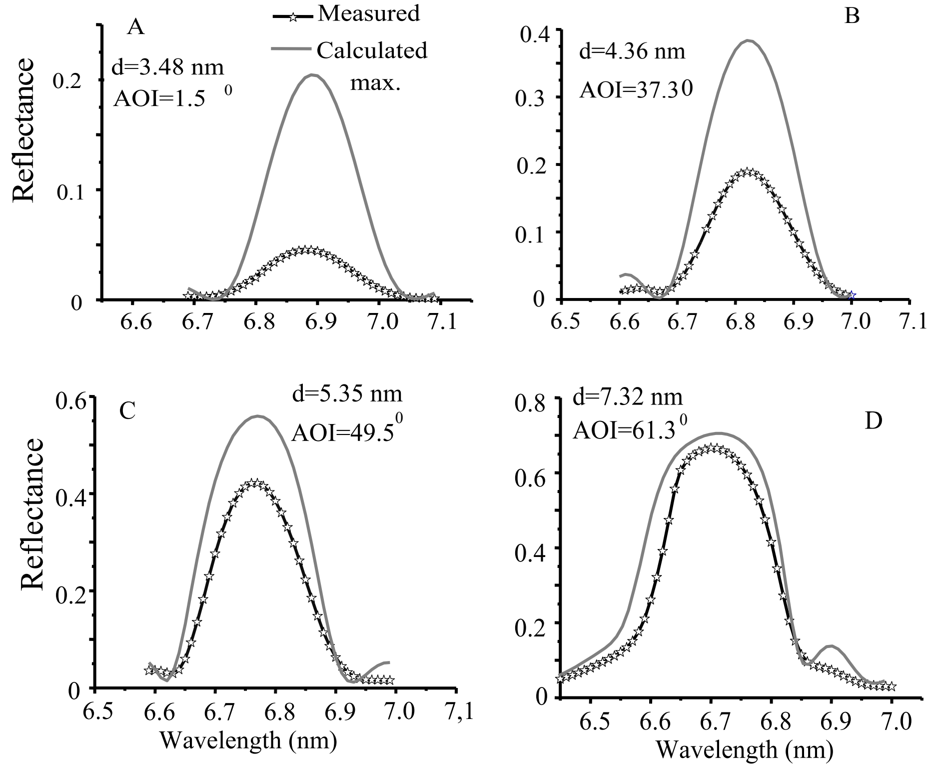

Fig. 1. Measured (markers) and simulated (lines) EUV reflectivity for e-beam deposited 40 period La/B multilayers with different periods. Simulations are performed using the parameters indicated in Table 1.

Table 1. Summary of Measured and Calculated Reflectance of La/B Multilayer Mirrors with Period Thicknesses from 3.45 to 7.25 nm at Indicated Angles of Incidence

Fig.	Λ, nm	AOI, degrees	R, %	R^0, %	Wavelength, nm
1A	3.49	1.5	4.5	20	6.89
1B	4.36	37.3	18.5	38	6.82
1C	5.35	49.5	42.1	56	6.76
1D	7.32	61.3	66.5	72	6.71

The important result of our analysis is that close to theoretical reflectance values can be obtained experimentally as shown in Fig. 1(d), confirming that La and B have sufficient optical contrast to achieve high reflectance providing the multilayer interface can be improved.

#197545 - $15.00 USD   Received 13 Sep 2013; revised 14 Nov 2013; accepted 20 Nov 2013; published 26 Nov 2013
(C) 2013 OSA

3 La/B and LaN/B multilayer structures

3.1 Experimental

In this paragraph we analyze the composition of a La/B and two differently produced LaN/B multilayer mirrors. The multilayers are deposited using the magnetron sputtering deposition method described by Yakshin et al. [17]. Here we selected magnetron sputtering because this technique is commonly used for the deposition of multilayer with large number of periods. Two different methods are used to nitridate the La layers: reactive magnetron sputtering of La in a mixture of Ar and N_2 (indicated by La(N)/B) and post treatment of the La layers by N_2-ions [2] (indicated by La/N/B). For our structural analysis we have deposited 50 bi-layers instead of the 175 required for maximum normal incidence EUV (NIER) reflectance because 50 period stacks suffer less from period variations. The period thickness is optimized for reflectance at 6.8 nm wavelength, close to but sufficiently far from the B-K absorption edge to avoid edge effects in the NIER curve.

The common way to reconstruct the multilayer mirror structure is to fit the grazing incidence hard X-ray reflectivity (GIXR) data, measured typically with $CuK_{\alpha 1}$ radiation. Fitting procedures assume minimization of a merit function by variation of the model parameters: interface roughness, layer density and layer thickness. However, due to the large amount of variable parameters for multilayer structures, the data fit will be complex. Moreover, it is impossible to prove that the obtained fit is the unique solution to the problem.

Combining GIXR and NIER fits increases the consistency of the fits not only because of the increasing amount of experimental data, but also because of the different optical response of the materials to the used hard and soft X-rays. Both measurements are sensitive to the electron density profiles of multilayer periods, but GIXR is less sensitive to the exact atomic composition of the layer (particularly the presence of lanthanum in boron) and the fit suffers less from correlation between structure parameters. Because of the large optical contrast for EUV light between spacer (here B) and reflector (here La) material, the NIER is sensitive to the atomic composition of the layers, particularly for the spacer layer.

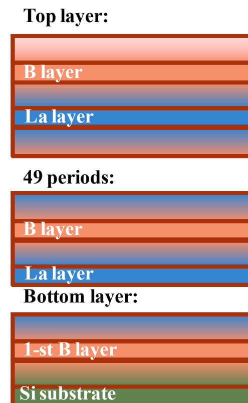

Fig. 2. The scheme of the model for grazing incidence hard X-ray reflectivity and normal incidence EUV reflectance data fitting.

#197545 - $15.00 USD Received 13 Sep 2013; revised 14 Nov 2013; accepted 20 Nov 2013; published 26 Nov 2013
(C) 2013 OSA

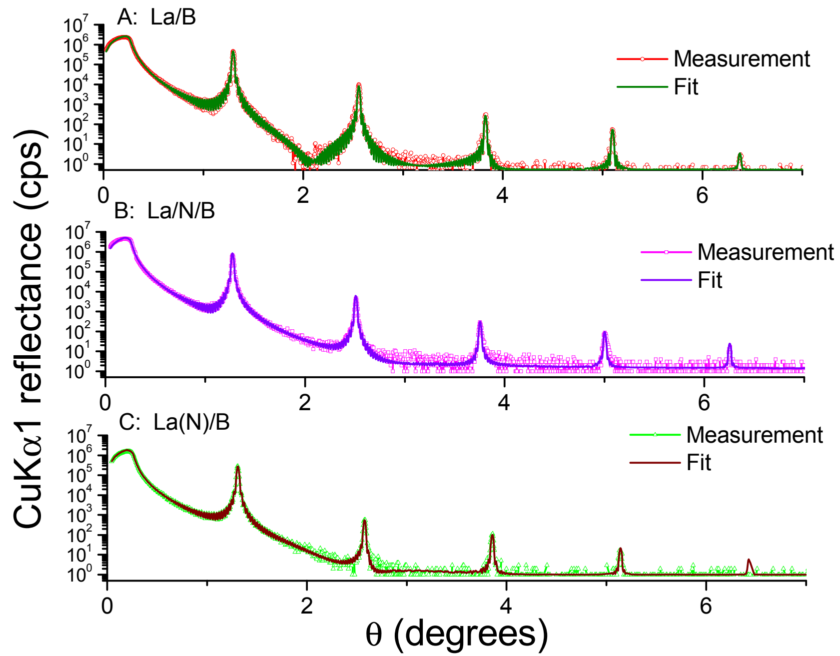

Fig. 3. Measured and calculated grazing incidence Cu-Kα1 reflectivity curves for La/B, La/N/B and La(N)/B multilayers.

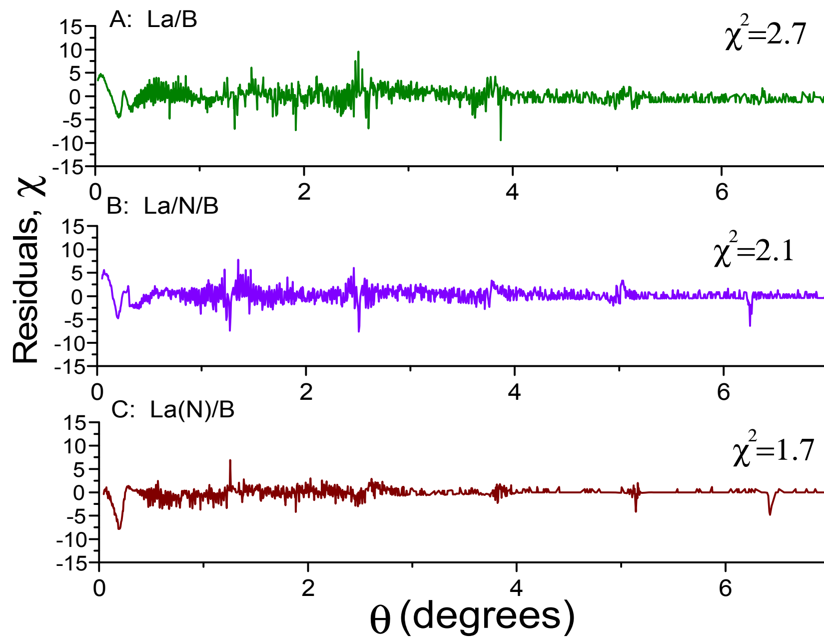

Fig. 4. Residuals between Cu-$K_{\alpha 1}$ measured and calculated data presented in Fig. 3.

#197545 - $15.00 USD Received 13 Sep 2013; revised 14 Nov 2013; accepted 20 Nov 2013; published 26 Nov 2013
(C) 2013 OSA

As a first step in the data analysis, we performed a GIXR data fit, minimizing χ^2_{GXIR}.The initial guess model for the GIXR data analysis was taken from the deposition design parameters. The best fit model from GIXR analysis was further used as an initial guess model for the simultaneous fit of GIXR and NIER that minimizes the sum $\chi^2_{GIXR} + \chi^2_{NIER}$. For fitting we are using the merit function given in Eq. (1).

$$\chi^2 = \frac{1}{L-l}\sum_{j=1}^{l}\frac{\left(I_j^{theory} - I_j^{\exp}\right)^2}{\sigma_{\exp}^2}, \tag{1}$$

Here I^{theory} and I^{exp}, are the calculated and measured intensities, σ_{exp} is the measurement error, L is the number of data points, l is the number of fit parameters. The Levenberg-Marquard [18] optimization algorithm was used for the minimization of χ^2.

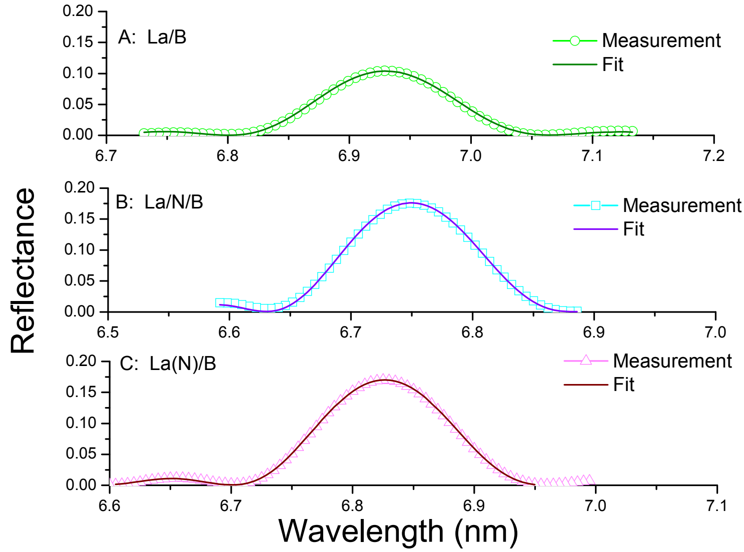

Fig. 5. Measured and calculated normal incidence EUV reflectivity spectra for 50 period La/B, La/N/B and La(N)/B multilayer stacks.

The data fit was carried out using the model of a multilayer structure presented in Fig. 2, assuming the multilayer to consist of a B-layer on a Si substrate, N-1 identical periods with N being the number of periods, and finally one bi-layer on the top of the stack. The substrate surface roughness, parameters of the first boron layer, period bi-layer and top bi-layer can be varied separately. The top layer and the substrate are mostly responsible for the reflectivity features observed between the Bragg diffraction peaks in the GIXR curves (Fig. 3) and our model should be able to fit this. Physically, parameters of the first boron layer and top period can be different from the periodic layers because of contact to substrate and air respectively. For each layer the layer thickness, density and interface thickness and the atomic composition can be varied during the fit. The interface roughness/diffusion regions are described by dividing the interface area in thin sub-layers with thickness of less than 0.1 nm, creating a linear profile in the optical contrast. This allows bypassing the discussion about the validity of the Debye-Waller or the Nevot-Crosse approximation to describe the GIXR and NIER data. For the calculation of reflectivity curves the transfer matrix formalism [19] was used. The details of data analysis procedure are described in ref [20].

Measurements and calculations of GIXR using the results of the simultaneous fits are presented in Fig. 3. To demonstrate the fit quality, the residuals in terms of $\chi_\theta = (I_\theta^{\ theory} - I_\theta^{exp})/\sigma_{exp}$ are displayed in Fig. 4 together with the value of χ^2. The small difference in the χ^2

#197545 - $15.00 USD Received 13 Sep 2013; revised 14 Nov 2013; accepted 20 Nov 2013; published 26 Nov 2013
(C) 2013 OSA

value indicates that the fits can be considered of equal quality. All Bragg maxima are described equally well and the difference in χ^2 values are mainly due to the regions in between the Bragg peaks where the top-bottom of the complete stack and layer aperiodicity are the major factors. The measured NIER spectra as well as the results of the simultaneous fit with the data of Fig. 3 are plotted in Fig. 5 showing a very good agreement. It should be noted that adding the layer stoichiometry to the fitting variables is vital to enable high quality simultaneous fitting of GIXR and NIER. Like in EUV reflectivity modelling in section two, measured La [21] and B [12] optical constants have been used.

3.2 Discussion

The results of the simultaneous fit of GIXR and NIER data of the La/B, La(N)/B and the La/N/B multilayers are summarized in Table 2 and in Fig. 6 that displays the reconstructed optical contrast profiles of these three multilayers. These profiles are represented by δ (δ = 1–n with n being the real part of the optical constants) and are calculated for 6.8 nm wavelength.

Figure 6 shows that the La/B multilayer has the lowest optical contrast which results in a reflectance of only 10.5% (Fig. 5). Furthermore, Table 2 shows that the B layer in the La/B stack has a high density of 2.9 g/cm^3 compared to its bulk value of 2.1 g/cm^3. This can be explained by the presence of 5 at.% La in the B layer. The La layer density of 5.2 g/cm^3 is rather low compared to the 6.17 g/cm^3 for bulk material, most likely caused by 63 at% of B in the La layers (see Table 2). The huge amount of B in La layer can be explained by dramatic intermixing of La and B. However, one should be careful with the obtained absolute value since the fit is not very sensitive to the B in La concentration. The La contamination in the B layer has a more dramatic effect on the optical contrast than B in La, therefore, the fit is much more sensitive to the presence of La in B than B in La. The interface asymmetry that is detected indicates that the B-on-La interface region is thicker than the La-on-B interface, which can be explained by island growth of the La layer leading to a thicker interface region when B grows on it. Table 2 shows that only 30% of the La/B period consists of layers with constant atomic composition and density, or in other words is not a part of the interface region. This also shows the relatively large intermixing.

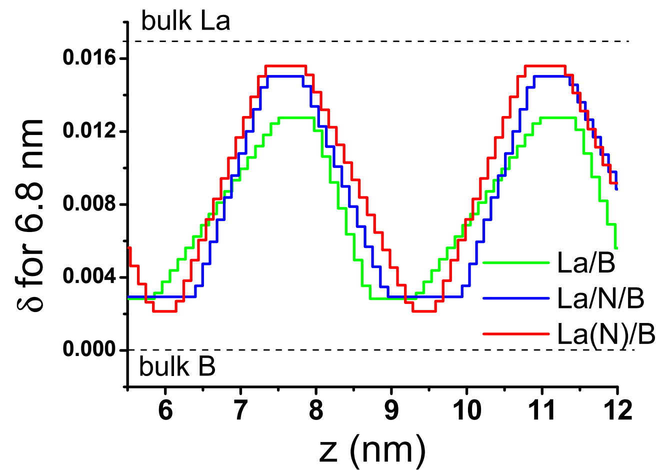

Fig. 6. Reconstructed optical profile for La/B, La/N/B and La(N)/B multilayer stacks calculated for 6.8 nm wavelength and presented as δ = 1-n where n is the real part of the dielectric permittivity.

The reconstructed profiles for both LaN/B stacks (Fig. 6) confirm that passivation of La with nitrogen, either by post N-ion treatment or by the reactive sputtering of La, increases the

#197545 - $15.00 USD Received 13 Sep 2013; revised 14 Nov 2013; accepted 20 Nov 2013; published 26 Nov 2013
(C) 2013 OSA

optical contrast by preventing the La-B interdiffusion or improving the layer growth properties. However for both multilayers the optical contrast is still lower than for LaN and B layers with bulk properties. According to Table 2 the density of the LaN layer in both multilayers is lower than the bulk value for the stoichiometric LaN which is 6.7 g/cm^3. This means that the LaN layer should either contain some B or pores to explain the layer density. Because of the small difference between boron and nitrogen optical constants compared to La, the fit is not sensitive to the exact atomic composition of the LaN layer as well as the presence of B in LaN layer. In the initial fitting model the atomic composition of the nitrided lanthanum layer was selected as LaN. During the fit it remains as initially assumed, LaN, for both stacks, La/N/B and La(N)/B, although the composition coefficients were free to vary.

Table 2. Summary of Structural Parameters for La/B, La/N/B and La(N)/B Multilayer Reconstructed Using Simultaneous Grazing Incidence X-ray Reflectivity and Normal Incidence EUV Reflectivity Fits

Sample	Layer thickness, nm	Interface linear transition width, nm (on top of the layer)	Density, g/cm^3	Layer compound stoichiometry in at %		
				La	*B*	*N*
La/B: R 10.5% @6.92 nm						
B layer	0.6	0.7	2.9	5	95	
La layer	0.5	1.6	5.2	37	63	
La/N/B R:17.5@6.75 nm						
B layer	1.0	1.1	2.5	0	79	21
La/N layer	0.5	1.0	5.1	50	0	50
La(N)/B R:17%@6.82 nm						
B layer	0.3	1.4	2.4	0	84	16
La(N) layer	0.5	1.2	5.3	50	0	50

Table 2 suggests that in the La/N/B multilayer the boron layers contain 21 at.% of N versus 16 at.% in the La(N)/B multilayer, resulting in a higher than bulk density. This can easily be understood in both cases: although the N-ion treatment in the La/N/B multilayer takes place only after deposition of the La, N-ions can easily penetrate the La and penetrate in the B-layer because of the low La thickness. This is confirmed by TRIM calculations for 150 eV N_2 . In the case of reactive magnetron sputtering for La(N) deposition the plasma creates also nitrogen ions and radicals that can interact with the sample surface as soon as the plasma is created. This creates boron-nitride simultaneously with the first arriving lanthanum particles, potentially changing growth conditions and modifying all important parameters for layer growth. The fact that La(N)/B has a slightly higher optical contrast than La/N/B can be explained by better growth conditions of LaN on B than in the case of La on B.

Both LaN/B multilayers do not show the asymmetry of the interfaces observed in the La/B stack. However no significant reduction of the total interface region is observed. The analysis of the La/N/B stack shows that the thickness of the layers with constant atomic composition and density is increased to about 40% of the period thickness but the La(N)/B multilayer has an even smaller non-interface region than the La/B multilayer. Comparing the two techniques to produce LaN, the only difference observed is that the reactive magnetron sputtering process used here produces a lower amount of nitrogen content in the boron layers at the expense of a slightly larger interface width. The smaller thickness of the interface regions in the La/N/B multilayer compensates the effect of the lower optical contrast compared to the La(N)/B multilayer and as a result both La/N/B and La(N)/B multilayers show comparable near normal incidence EUV reflectance for the analysed 50 period multilayer mirrors. The next step in the development of the stack deposition technology could be the combination of the reactive La sputtering with N-ion post treatment.

#197545 - $15.00 USD Received 13 Sep 2013; revised 14 Nov 2013; accepted 20 Nov 2013; published 26 Nov 2013
(C) 2013 OSA

4. High reflectance coatings

In order to demonstrate high reflectance for lanthanum-boron multilayers, the best candidates from the previous set have been scaled up. La(N)/B and La/N/B multilayer mirrors consisting of 175 periods have been deposited to evaluate the achievable normal incidence reflectance around 6.7 nm wavelength. The EUV reflectivity measurements have been performed, similar to measurements for 50 period coatings, at 1.5 degree off normal using s-polarized light.

The measured reflectivity results are presented in Fig. 7 together with simulations based on the model parameters obtained for the 50 period multilayer described in the previous section. No additional fits have been performed. The only difference with the previous section is the number of periods and the period thickness that had to be slightly scaled to match the wavelength of ~6.65 nm. It should be noticed that the model reconstructed for 50 period coating does not take any aperiodicity or roughness evolution during the multilayer growth into account.

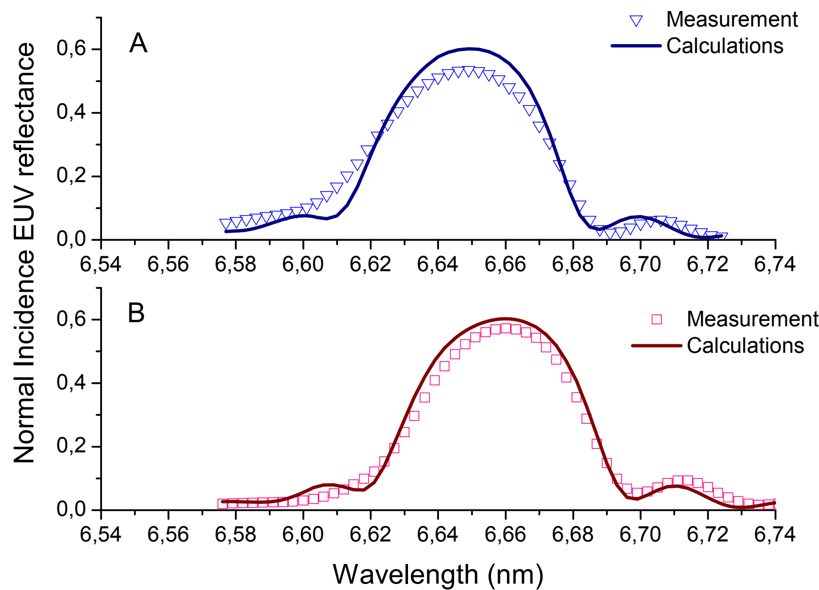

Fig. 7. Normal incidence EUV reflectivity spectra for 175 period La/N/B (A) and La(N)/B (B) multilayer mirrors measured and calculated using models reconstructed for 50 period stacks.

Figure 7 shows that a reflectance for La/N/B of 53% has been measured versus 57.3% for the La(N)/B multilayer mirror. The measured reflectivity is in both cases smaller than the 60% value predicted by the simulations. The reflectance curve of the La/N/B multilayer [Fig. 7(a)] shows a significantly larger width than the calculated curve as well as the measurement of the La(N)/B multilayer [Fig. 7(b)]. This increase in the La/N/B reflectance peak width and the slightly larger Kiessig fringe oscillations can be simulated by a decrease in the number of periods from 175 to 145, hinting more in the direction of aperiodicity in the stack. The predicted reflectance is met best by the La(N)/B multilayer mirror indicating that the La(N)/B multilayer deposition has lower aperiodicity and no significant evolution of interface roughness. The higher aperiodicity of La/N/B multilayer can be explained by the difference in the deposition process. The post N-ion treatment is an additional step in the deposition process and may cause extra instability of the growth process that is best visible for a coating with large number of periods.

However, in both cases the difference between the obtained and predicted reflectance is not dramatic and optimisation of the deposition technology should be able to correct for this.

#197545 - $15.00 USD Received 13 Sep 2013; revised 14 Nov 2013; accepted 20 Nov 2013; published 26 Nov 2013
(C) 2013 OSA

5. Conclusions

Experiments with large period multilayers for off normal reflectance of 6.8 nm radiation have demonstrated that the material combination of La with B shows sufficient optical contrast to obtain almost theoretical reflectance values if the influence of interface roughness can be reduced.

Analysis of short period La/B multilayer structures for normal incidence reflectance of 6.8 nm light has revealed that the multilayer has a low optical contrast that is most likely caused by intermixing between the layers. In order to prevent this intermixing two techniques of nitridation of La, namely post N-ion treatment of the thin La layer and reactive La sputtering in a N_2 atmosphere have been applied to deposit LaN/B multilayers. The nitridation of La in both cases increases the optical contrast between La and B significantly and consequently increases the EUV reflectivity. The nitridation does however not change the total width of the interfaces, leaving ample room for further improvements.

The optical contrast of LaN/B multilayer stacks is also limited by the presence of N atoms in the B layers and should be reduced by further improvement of the nitridation process. The highest normal incidence reflectivity of 57.3% at 6.65 nm was measured from the 175 period La(N)/B multilayer stack. The measured reflectivity is slightly less than the calculated value of 60% that is based on the reconstructed multilayer structure. The difference can be explained by a minor error in periodicity or roughness growth for large number of periods, but no major changes of structure caused by the multilayer growth process is expected.

Acknowledgments

This work is part of the project ‘Multilayer Optics for Lithography Beyond the Extreme Ultraviolet Wavelength Range’ carried out with support of the Dutch Technology Foundation (STW). This work is also a part of ‘Controlling photon and plasma induced processes at EUV optical surfaces (CP3E)’ of the ‘Stichting voor Fundamenteel Onderzoek der Materie (FOM)’ with financial support from the ‘Nederlandse Organisatie voor Wetenschappelijk Onderzoek (NWO)’, Carl Zeiss SMT, ASML, and the AgentschapNL through the EXEPT program.

130.89.46.45 {ts '2019-01-30 06:05:45'}